PNAS
www.pnas.org

Supplementary Information for

Plastocyanin is the long-range electron carrier between photosystem II and photosystem I in plants

Ricarda Höhner[1], Mathias Pribil[2,3,#], Miroslava Herbstová[4], Laura Susanna Lopez[1], Hans-Henning Kunz[5], Meng Li[1], Magnus Wood[1], Vaclav Svoboda[1], Sujith Puthiyaveetil[1,6], Dario Leister[3,&], Helmut Kirchhoff[1,*]

[1], Institute of Biological Chemistry, Washington State University, PO Box 646340, Pullman, WA, 99164-6340, USA.

[2], Copenhagen Plant Science Centre, Department of Plant and Environmental Sciences, University of Copenhagen, Thorvaldsensvej 40, DK-1871 Frederiksberg C, Copenhagen, Denmark.

[3], Plant Molecular Biology (Botany), Department Biology I, Ludwig-Maximilians-Universität München, 81252 Planegg-Martinsried, Germany.

[4], Institute of Plant Molecular Biology, Biology Centre CAS, Branišovská 1160/31, 37005 České Budějovice, Czech Republic.

[5], School of Biological Sciences, Washington State University, PO Box 644236 Pullman, WA 99164-4236, USA.

[6], Current address: Department of Biochemistry and Center for Plant Biology, Purdue University, West Lafayette, IN 47907.

Helmut Kirchhoff
Email: kirchhh@wsu.edu

This PDF file includes:

www.pnas.org/cgi/doi/10.1073/pnas.2005832117

SI Fig. 1

SI Fig. 1. Growth phenotype of WT and plants with altered CURT1 protein levels. Shown are 8-week-old plants. The weight numbers on the bottom represent the above ground biomass from four biological repeats.

SI Fig. 2

Electron transport model for the high potential chain

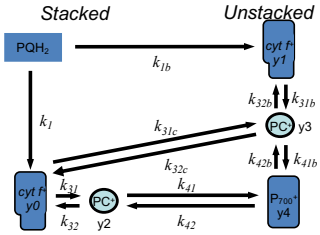

$K_{eq}F\_Pc$	1.8
$K_{eq}Pc\_P$	23
k1	210 s^{-1}
k1b	1 s^{-1}
k31	31 s^{-1}
k31b	31 s^{-1}
k31c	31 s^{-1}
k32	17.2 s^{-1}
k32b	17.2 s^{-1}
k32c	17.2 s^{-1}
k41	71 s^{-1}
k41b	71 s^{-1}
Ptot	2 mM total PSI conc.
Ftot	1 mM total cyt f conc.
Pctot	3.6 mM total PC conc.
Fpart	0.5 fraction cyt $b_6f_{stacked}$
Pcpart	0.5 fraction $PC_{stacked}$

Differential equations

Concentration of reduced cyt f stacked (y0):

$$\frac{dy_0}{dt} = k1 \cdot (F_{stack} - y_0) - k31 \cdot (PC_{stack} - y2) \cdot y0 + k32 \cdot (F_{stack} - y0) \cdot y2 - k31c \cdot (PC_{unstack} - y3) \cdot y0 + k32c \cdot (F_{stack} - y0) \cdot y3$$

Concentration of reduced cyt f unstacked (y1):

$$\frac{dy_1}{dt} = k1b \cdot (F_{unstack} - y1) - k31b \cdot (PC_{unstack} - y3) \cdot y1 - k32b \cdot (F_{unstack} - y1) \cdot y3$$

Concentration of reduced plastocyanin stacked (y2):

$$\frac{dy_2}{dt} = k31 \cdot (PC_{stack} - y2) \cdot y0 + k32 \cdot (F_{stack} - y0) \cdot y2 - k41 \cdot (P700 - y4) \cdot y2 + k42 \cdot (PC_{stack} - y2) \cdot y4$$

Concentration of reduced plastocyanin unstacked (y3):

$$\frac{dy_3}{dt} = k31b \cdot (PC_{unstack} - y3) \cdot y1 + k32b \cdot (F_{unstack} - y1) \cdot y3 - k41b \cdot (P700 - y4) \cdot y3 + k42 \cdot (PC_{unstack} - y3) \cdot y4 + k31c \cdot (PC_{unstack} - y3) \cdot y0 - k32c \cdot (F_{stack} - y0) \cdot y3$$

Concentration of reduced P700 (y4):

$$\frac{dy_4}{dt} = k41 \cdot (P700 - y4) \cdot y2 - k42 \cdot (PC_{stack} - y2) \cdot y4 + k41b \cdot (P700 - y4) \cdot y3 - k42 \cdot (PC_{unstack} - y3) \cdot y4$$

Redox midpoint potential and equilibrium constants (K_{eq})

	ΔE_m	Literature	Value used	K_{eq}
Rieske	310 mV 320 mV 280-320 mV	Hope 1993 Hope 1993 Malkin 1981, Nitschke 1992	310 mV	Rieske-Cyt f: 6.0
Cyt. f	358 mV 355 mV 350 mV 350-370 mV 340-360 mV	Hope 1993 Hope 1993 Hope 1993 Drepper 1994 Kirchhoff et al. 2004	355 mV	Cyt f – PC: 1.8
PC	355-370 mV 360-380 mV	Kirchhoff et al. 2004 Drepper 1994	(370 mV)	(78.4)
PC bound to PSI	421 mV	Kirchhoff et al. 2004	(421 mV)	(10.4) 23*
P700	465-485 mV 468-492 mV	Kirchhoff et al. 2004 Drepper 1994	480 mV	

* Taken from the apparent PC/P700 K_{eq} measured for WT.

Rate constants

	$k_{forward}$	$k_{backward}$	Literature	Value used
PQH2 => Rieske	< 0.3 ms^{-1} 0.30 ms^{-1} 0.27 ms^{-1}	No back reaction	Cramer et al. 1996 Hope 2003 Selak and Whimarsh 1982	k1 = 0.21
Rieske ⇔ cyt f	fast	From K_{eq}	Hope 1993	k21 = 1000
Cyt f ⇔ PC	1.7*10^7 M^{-1} s^{-1} 4.5*10^7 M^{-1} s^{-1}	From K_{eq}	Sujak et al. 2004 Hope 2000	k31 = 3.1*10^7
PC ⇔ P700	9.2*10^7 M^{-1} s^{-1} 5.0*10^7 M^{-1} s^{-1}	From K_{eq}	Hippler et al. 1998 Hope 1993	k31 = 7.1*10^7

Simulated $P700^+$ and cyt f^+ rereduction kinetics for diffusion restriction of PC or PQH_2 in *curt1abcd*

PC-diffusion restriction: deceleration of *k31, k31c, k41, k41*c by factor 0.0024
PQ-diffusion restriction: deceleration of *k1* by factor 0.67
Deceleration factors determined to describe $P700^+$ kinetics.

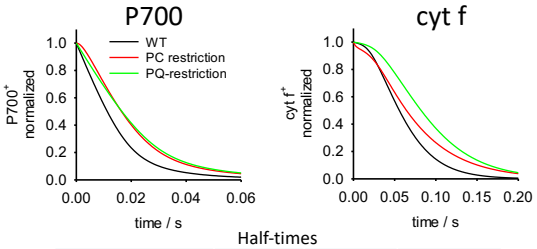

Half-times

	WT	*curt1abcd*	ratio *curt1abcd* / WT
P700 meas.	11.3+/-1.0ms	16.6+/-2.3ms	1.47
P700 sim, WT	11.3ms	-	
P700 sim, PC-restr.	-	16.5ms	1.47
P700 sim, PQ restr.	-	16.6ms	1.47
Cyt f meas.	57.2+/-7ms	66.6+/-8ms	1.16
Cyt f sim, WT	55.8ms	-	
Cyt f sim, PC-restr.	-	64.4ms	1.15
Cyt f sim, PQ restr.	-	82.2ms	1.47

SI Fig. 2. Mathematical model describing electron transport from PQH_2 to $P700^+$. The differential equations on the upper right describe the re-reduction of the cyt f^+, PC^+, and $P700^+$ after a MT light pulse that reduces the PQ-pool mimicking the experiment in Fig. 4a (top). The model assumes two populations of cyt b_6f complexes and PC localized to stacked and unstacked thylakoid regions, respectively (upper left). Rate constants and numbers used for the model are defined in the cartoon in the upper left. The tables to the lower left survey redox midpoint potentials and rate constants for these reactions. The outcome of the model for P700 and cyt *f* reduction kinetics for WT and *curt1abcd* is shown in the lower right for no restrictions in PQ- and PC-diffusion (black lines, WT), a PQ-diffusion restriction scenario (green lines) and for the case of PC-diffusion restriction (red lines). The half times for $P700^+$ and cyt f^+ derived from these kinetics are shown in the table at the bottom and are compared to measure data. Note that the apparent inhibition for cyt f^+ reduction is best described for the PC-diffusion restricted case (see numbers highlighted in red).

SI Fig. 3

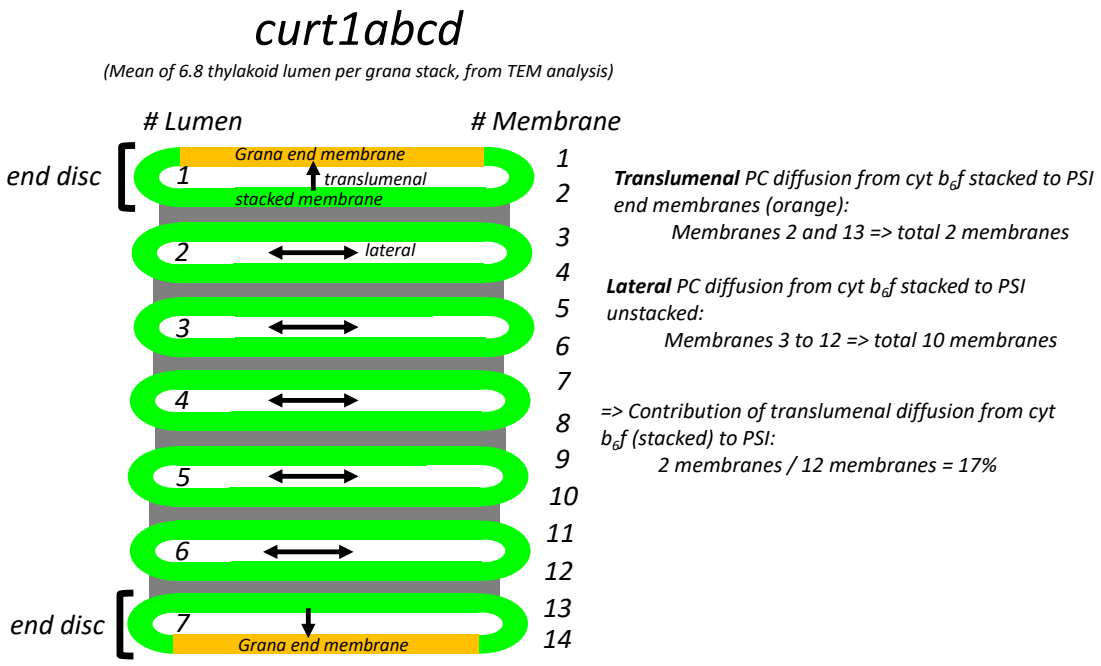

SI Fig. 3. Estimation of the contribution of transluminal PC-diffusion in grana end discs to connect cyt b_6f complexes in stacked thylakoids to PSI for *curt1abcd*. The number of grana discs for *curt1abcd* were derived from TEM images. Translumenal PC-diffusion for end discs #1 and #7 is expected to be fast because of shorter diffusion distances (vertical instead of lateral) and lesser crowding of the lumen (PSII abundance low in end membranes). The model estimates the fraction of cyt b_6f complexes localized in the stacked membranes #2 and #13 that are involved in translumenal PC diffusion relative to all cyt b_6f complexes in stacked domains (connected to PSI by lateral and transluminal PC-diffusion). The assumption is that all stacked membranes (#s2-13) have the same cyt b_6f concentration. The calculations to the right estimate that in stacked grana <20% of cyt b_6f complexes are involved in fast translumenal diffusion in *curt1abcd*.

SI Fig. 4

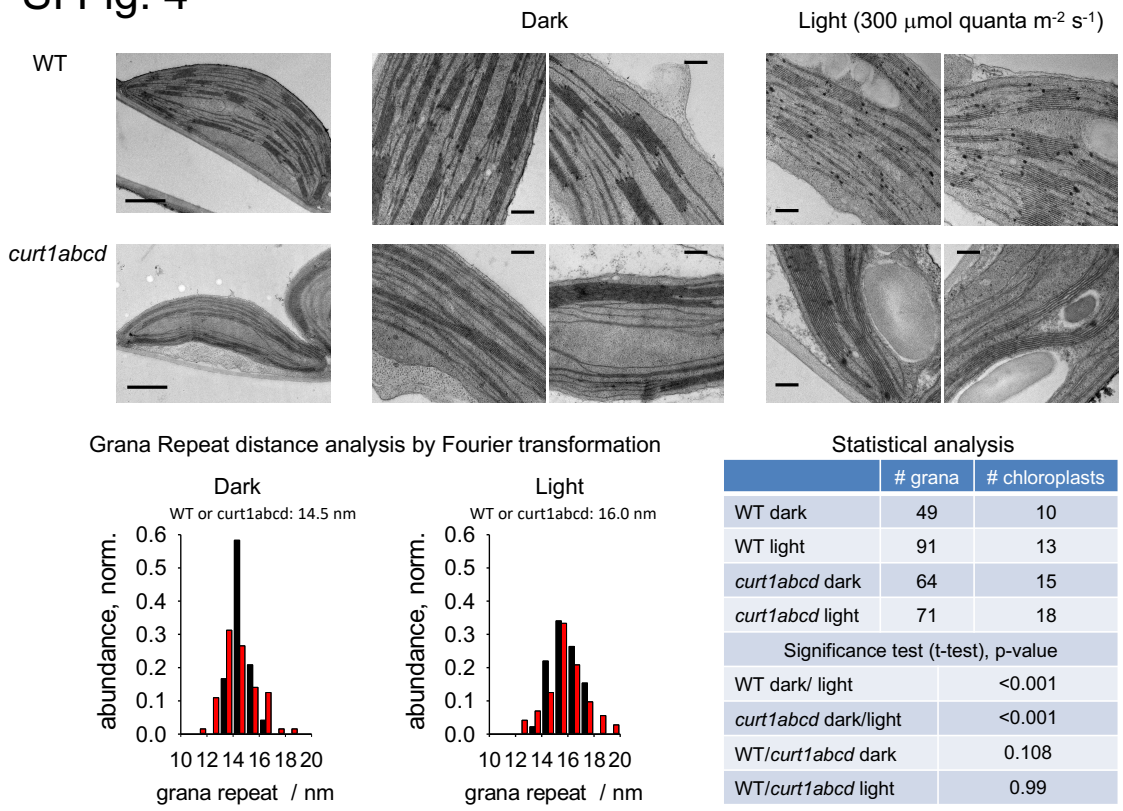

Statistical analysis

	# grana	# chloroplasts
WT dark	49	10
WT light	91	13
curt1abcd dark	64	15
curt1abcd light	71	18
Significance test (t-test), p-value		
WT dark/ light	<0.001	
curt1abcd dark/light	<0.001	
WT/*curt1abcd* dark	0.108	
WT/*curt1abcd* light	0.99	

SI Fig. 4. Transmission electron microscopy (TEM) on leaf discs for WT (upper panel) and *curt1abcd* (lower panel). TEM examples for dark and light-adapted plants (20 min) are shown. The stacking repeat distances between two lumen in grana was determined by Fourier transformation as described in (Kirchhoff et al. 2011). Results and statistical analysis for dark- and light-adapted conditions are presented at the lower panel. Scale bars: Images to the left, 1000 nm, images middle and right, 200 nm. The analysis revealed that *curt1abcd* perform the same light-induced swelling of the thylakoid lumen as the WT. The absolute number of lumen swelling is smaller than reported in Kirchhoff et al. 2011 likely because of the lower light intensity used in this study (300 versus 500 µmol quanta m^{-2} s^{-1}).

SI Fig. 5

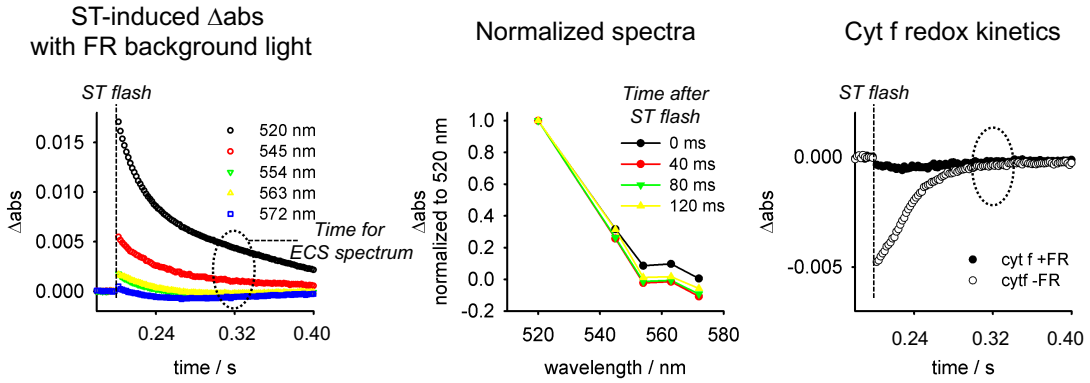

SI Fig. 5. Determination of the ECS contribution at 554 nm (cyt *f*) after baseline correction (545 nm to 572 nm). The graph to the left shows absorption changes induced by a ST flash in leaves illuminated with weak FR background light. The FR background light pre-oxidizes cyt *f*, i.e. the kinetics (left) are dominated by the ECS and not by cyt *f*. The indicated time interval (around 0.32 s) was used to extract the ECS specific absorption change (middle) since at this time interval the remaining cyt *f* redox change relaxed completely (black circles, right).

Table S1: Survey of recent published ultrastructural data on the grana diameter for different higher plant species.

Technique	**Grana diameter**	**Reference**	**Plant material**
Scanning –EM	500+/-28 nm	Kaftan et al. 2005	Lettuce
AFM	450+/-30 nm	Kaftan et al. 2005	Lettuce
Thin-section EM	410+/-10 nm 470+/-10 nm	Armbruster et al. 2013	Arabidopsis
Thin-section EM	439+/-155 nm	Fristedt et al. 2009	Arabidopsis
Thin-section EM HPF	ca. 480 nm	Pfeiffer & Krupinska 2005a	Barley
Thin-section EM HPF	400-420 nm	Pfeiffer & Krupinska 2005b	Stinging-nettle (Urtica dioica L.)
EM tomography	350-550 nm	Daum et al. 2010	Spinach
EM tomography	ca. 410 nm	Kouril et al. 2011	Spinach
3D-SIM	400-600 nm	Wood et al. 2019	Spinach
Mean	**410-495 nm**		

Table S2: Compositional characterization of intact thylakoid membranes and thylakoid subtractions.

	WT	***curt1abcd*-ko**	**CURT1A-oe**
[a)]mmol PSII / (mol Chl) thylakoid	2.46+/-0.32	2.64+/-0.30	2.48+/-0.20
[a)] mmol PSII / (mol Chl) stacked	3.91+/-0.10	3.65+/-0.07	3.72+/-0.12
[a)] mmol PSII / (mol Chl) unstacked	1.99+/-0.15	2.61+/-0.08*	2.15+/-0.21
[b)]mmol cyt b_6f / (mol Chl) thylakoid	0.90+/-0.12	0.80+/-0.10	0.84+/-0.07
[b)]mmol cyt b_6f / (mol Chl) stacked	0.59+/-0.06	0.47+/-0.03	0.54+/-0.05
[b)]mmol cyt b_6f / (mol Chl) unstacked	1.37+/-0.16	2.00+/-0.13**	1.90+/-0.26
[c)]mmol PC/ (mol PSI) thylakoid	4.1+/-0.2	4.4+/-0.1	4.2+/-0.1
Chl a/b thylakoid	3.17+/-0.03	3.01+/-0.04**	3.17+/-0.06
Chl a/b stacked	2.46+/-0.02	2.48+/-0.11	2.55+/-0.12
Chl a/b unstacked	4.30+/-0.24	4.94+/-0.60	5.21+/-0.50

a) Determined by difference absorption spectroscopy of cyt b559.

b) Determined by difference absorption spectroscopy of cyt f and cyt b6.

c) Calculated from maximal difference absorption changes at 820 nm and (820nm-920nm) according to Kirchhoff et al. 2004.

Data represent the mean with SEM of 3 to 11 biological repetitions. *, p-value < 0.05; **, p-value < 0.01

SI References

1. Kirchhoff, H., et al. Dynamic control of protein diffusion within the granal thylakoid lumen. *Proc Natl Acad Sci U S A* 108, 20248-20253(2011).

2. Armbruster U, Labs M, Pribil M, Viola S, Xu W, Scharfenberg M, Hertle AP, Rojahn U, Jensen PE, Rappaport F, Joliot P, Dörmann P, Wanner G, Leister D. (2013) Arabidopsis CURVATURE THYLAKOID1 proteins modify thylakoid architecture by inducing membrane curvature. *Plant Cell* 25, 2661-2678

3. Daum B, Nicastro D, Austin II J, McIntosh R, Kühlbrandt W (2010) Arrangement of photosystem II and ATP synthase in chloroplast membranes of spinach and pea. *Plant Cell* 22: 1299-1312

4. Fristedt R, Willig A, Granath P, Crevecoeur M, Rochaix JD, Vener AV (2009) Phosphorylation of photosystem II controls functional macroscopic folding of photosynthetic membranes in Arabidopsis. *Plant Cell* 21, 3950–3964

5. Kaftan D, Brumfeld V, Nevo R, Scherz A, Reich Z (2002) From chloroplasts to photosystems: in situ scanning force microscopy on intact thylakoid membranes. *EMBO J.* 21, 6146-6153

6. Kouril R, Oostergetel GT, Boekema EJ (2011) Fine structure of granal thylakoid membrane organization using cryo electron tomography. *Biochim. Biophys. Acta* 1807, 368–374

7. Pfeiffer S, Krupinska K (2005a) New insights in thylakoid membrane organization. *Plant Cell Physiol*. 46, 1443–1451

8. Pfeiffer S, Krupinska K (2005b) Chloroplast ultrastructure in leaves of Urtica dioica L. analyzed after high-pressure freezing and freeze-substitution and compared with conventional fixation followed by room temperature dehydration. *Microscopy Research Technique* 68, 368–376

9. Wood WHJ, Barnett SFH, Flannery S, Huner CN, Johnson MP (2019) Dynamic thylakoid stacking is regulated by LHCII phosphorylation but not its interaction with PSI. *Plant Physiol*. 180, 2151-2166.

10. Kirchhoff H, Schoettler MA, Maurer J, Weis E. (2004) Plastocyanin redox kinetics in spinach chloroplasts: evidence for disequilibrium in the high potential chain. *Biochim.*

Biophys. Acta 1659, 63-72